"Elucidating Pharmacokinetics profiles of *Hibiscus rosasinensis* Phytochemicals: A Computational approach for Drug Design in Diabetes"

Prakriti Maurya[1]*, Salil Tiwari[2], Amrita Yadav[3], Pawan Verma[4]
[1*]*Department of Pharmaceutical Chemistry, GIPS, Luck now, UP, India, Pin -226028*
[2]*Department of Pharmaceutical Chemistry, GIPS, Luck now, UP, India, Pin - 226028*
[3]*Department of Pharmaceutical Chemistry, GIPS, Luck now, UP, India, Pin - 226028*
[4]*Department of Pharmaceutical Chemistry, GIPS, Luck now, UP, India, Pin - 226028*
**Corresponding Author Email Id: pkt99maurya@gmail.com*

Abstract

Insulin resistance and a progressive reduction in insulin secretion cause diabetes mellitus; a complicated metabolic disease. Hibiscus rosasinensis, a medicinal plant with antidiabetic impacts, related to the Malvaceae family of plants. This study's objective was to use molecular docking to look at how the phytochemical parts of Hibiscus rosasinensis interact with various large molecules that are targets diabetes drugs. The intent of the current investigation was to assess the toxicity, pharmacokinetics, interaction, and receptor-ligand binding energy of certain phytocompounds against diabetes using molecular docking. This in silico study used the online tools Swiss ADME and Autodock (Version 4.2.6) to perform pharmacokinetics, bioavailability, drug-likeness, and toxicity prediction, as well as molecular docking. Additionally, molecular docking investigations against TCF7L2 were carried out. Consequently, using a variety of in silico techniques, the molecular docking of the thirty-three phytoconstituents was evaluated in this study against the TCF7L2 protein. The greatest binding affinity protein targets for TCF7L2 were found to be beta-sitosterol (-8.04 kcal/mol), strigast-5-ene-3beta, 4alpha-diol (-7.28 kcal/mol), flavylium (-6.97 kcal/mol), and quercetin (-6.62 kcal/mol).beta-Sitosterol, Stigmast-5-ene-3beta, 4alpha-diol and alpha-Carotene have best binding energy but low GI Absorption. Quercetin have high GI absorption but toxic if swallowed. Based on a study that predicts toxicological endpoints, median fatal dosage ranges (48 -23000). Subsequent analysis factors revealed Flavylium, Quercetin and thiamine had encouraging characteristics and might serve as a viable therapeutic candidate. Further in vivo and in vitro research to determine the most suitable medicinal molecule would be based on the predictions regarding the pharmacokinetic features of these phytoconstituents.

Keywords: *Diabetes Mellitus, TCF7L2, Hibiscus rosa sinensis, Pharmacokinetic, ADMET, Molecular docking.*

INTRODUCTION

Insulin resistance and increasing loss of insulin secretion are the causes of diabetes, a complicated metabolic illness. The endocrine condition known as diabetes is typified by decreased insulin secretion, harm to the pancreatic β-cells, problems with the metabolism of carbohydrates, fats, and proteins, and an additional elevated risk of consequences from other vascular disorders [1]. As a result, there is an increased risk of high blood sugar levels and heart disease, stroke, kidney disease, nerve damage, and blindness, among other serious illnesses. Type 1 and type 2 diabetes are the two primary forms of the disease [2]. Typically, children and young people are diagnosed with type 1 diabetes. This is the result of minimal or absent insulin production by the pancreas. Compared to type 1, type 2 diabetes is significantly more prevalent. Insulin resistance, or insufficient insulin production by the pancreas or improper insulin use by the cells, is a condition associated with type 2 diabetes [3]. According to WHO estimations, by 2030, 350–400 million individuals would have type 2 diabetes.10% of the population suffers from diabetes, a chronic and fatal illness brought on by an insufficient amount of insulin [4].

The most powerful locus for type 2 diabetes (T2D) risk is TCF7L2, which has also been the first to be reliably reported by genetic linkage studies. A fundamental component of the Wnt signaling pathway is the transcription factor TCF7L2 [5]. Understanding the function of TCF7L2 in the control of blood sugar levels, insulin secretion, and its effect will be aided by the physiological characterization of TCF7L2 risk polymorphisms for type 2 diabetes. A significant medicinal plant, *H. Rosa-sinensis* is a member of the Malvaceae family [6]. Chinese rose, or Hibiscus rosasinensis, is a highly significant medicinal plant that grows across India and the tropical and subtropical regions of the world [7]. The flowers have diaphoretic and emmenagogue properties, and they are used to halting heavy menstrual bleeding. Epilepsy, leprosy, pneumonia, and diabetes can all be effectively treated with them [8]. Analgesic, antidiabetic, healing, and antimutagenic activities are seen in the leaves [10], while the roots show hypolipidemic, antifertility, and neuroprotective qualities [9].

Currently, molecular docking is widely used to envision the ethics of small molecules (drug candidates) when they bind to their biomolecular target, which includes proteins, carbohydrates, and nucleic acids, in order to estimate their preliminary binding characteristics. Pharmacokinetic features (ADMET) were also examined using these techniques in addition to pharmacodynamic data (e.g., potency, affinity, efficacy, and selectivity) [11].When compounds binding affinities can be effectively anticipated by computational approaches prior to conducting trials, the overall cost of medication development is greatly decreased[12]. The production of ligands, determination of the binding energy of the protein-ligand complex, analysis of the data, and creation of 3-D structure of proteins are the several processes of molecular docking approach [13].

MATERIALS & METHODS

System configuration

Hardware that we used in this study was HP computer Device name-DESKTOP-1963BDB with Processor Intel(R) Celeron(R) CPU B830 @ 1.80GHz, RAM 6.00 and 64-bit operating system,x64-based processor. The Windows specification have Windows 10 Pro edition and 22H2 version.

Retrieval of Phytochemical Bioactive Compounds

The phytochemical bioactive compounds of *Hibiscus rosa sinensis* were retrieved from IMPPAT and their SMILE, PubChem ID, molecular formula, and 3D sdf file were retrieved from PubChem[14].

Molecular Structures

The molecular structure of the pytochemicals of *Hibiscus rosasinensis* are studied which are resprsented in Figure 1.1. The chemsketch tool are used for the two dimensional structure of the phytochemicals of *Hibiscus rosa sinensis* by using SMILE.

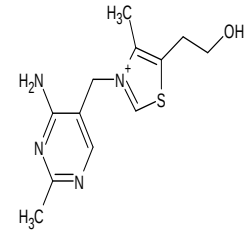

Thiamine

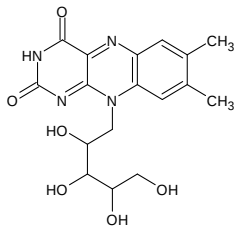

Riboflavin

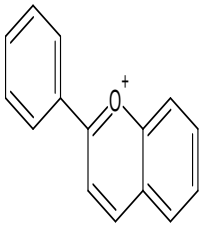

Flavylium

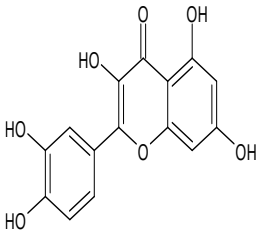

Quercetin

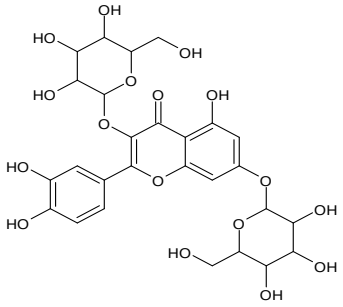

Quercetin-3,7-diglucoside

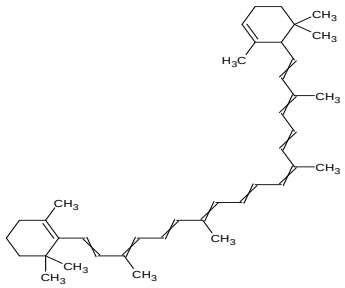

alpha-Carotene

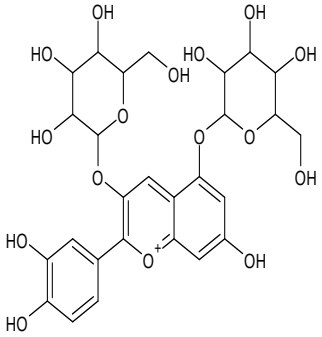

Cyanin

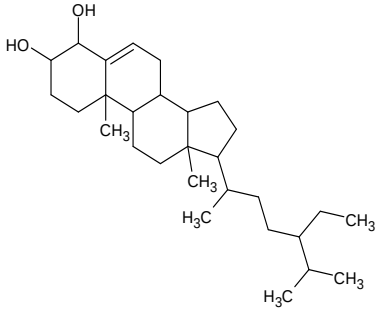

Stigmast-5-ene-3beta, 4alpha-diol

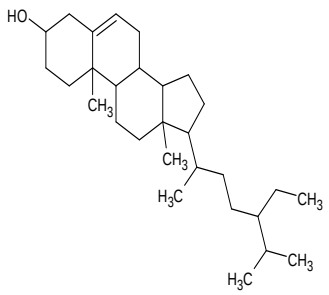

beta-Sitosterol

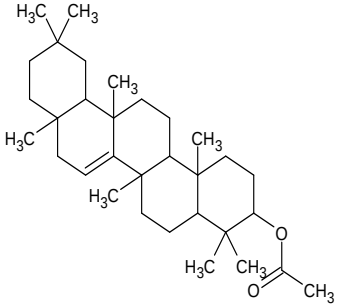

Taraxerol acetate

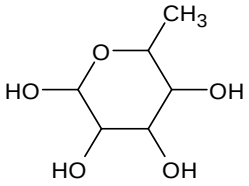

L-Rhamnose

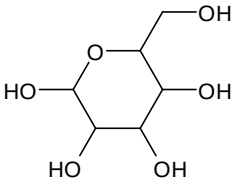

D-Galactose

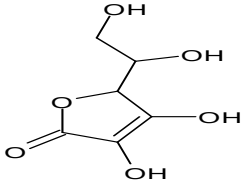

Ascorbic acid

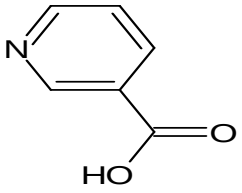

Nicotinic acid

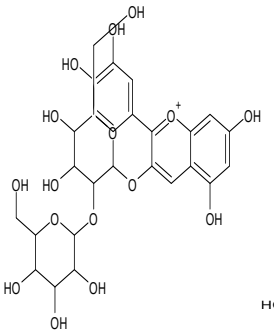

Cyanidine 3 -sophoroside

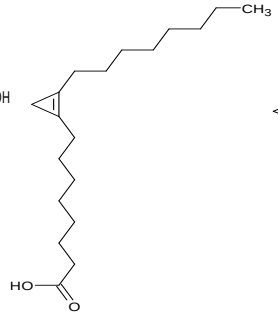

Sterculic acid

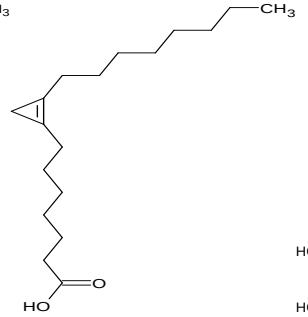

Malvalic acid

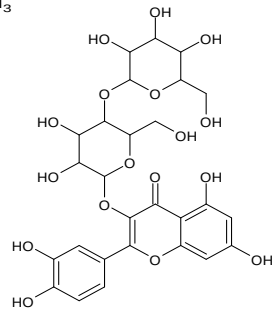

Quercetin 3-diglucoside

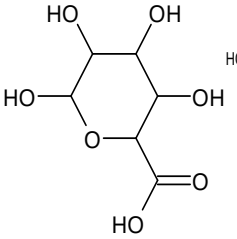

D-Glucuronic acid

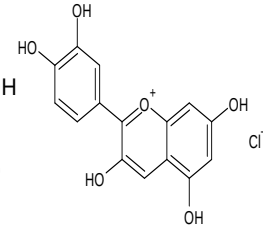

Cyanidin chloride

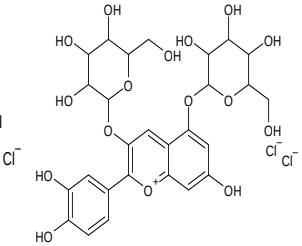

Cyanin chloride

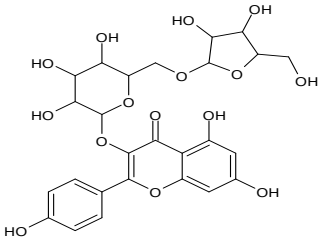

Kaempferol 3-xylosyl glucoside

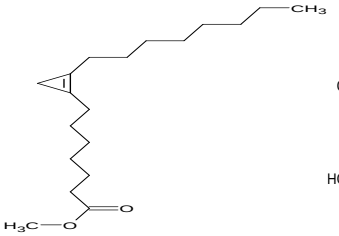

Methyl malvalate

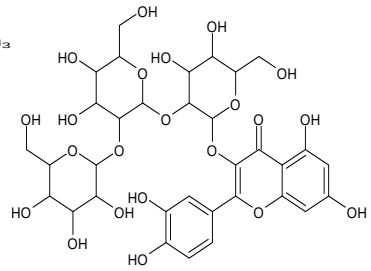

Quercetin 3-sophorotrioside

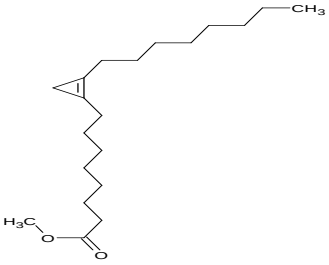

Methyl sterculate

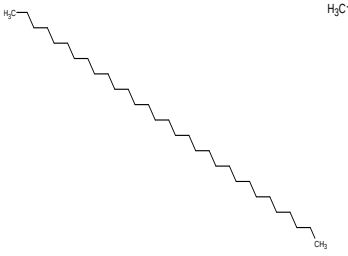

Hentriacontane

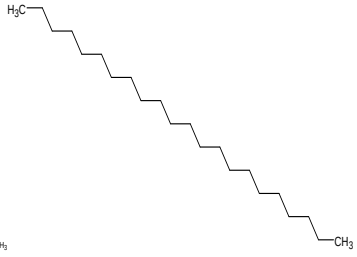

Docosane

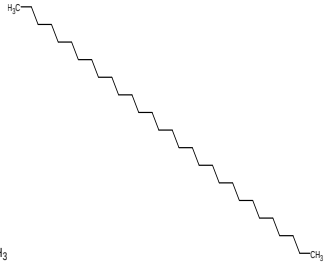

Triacontane

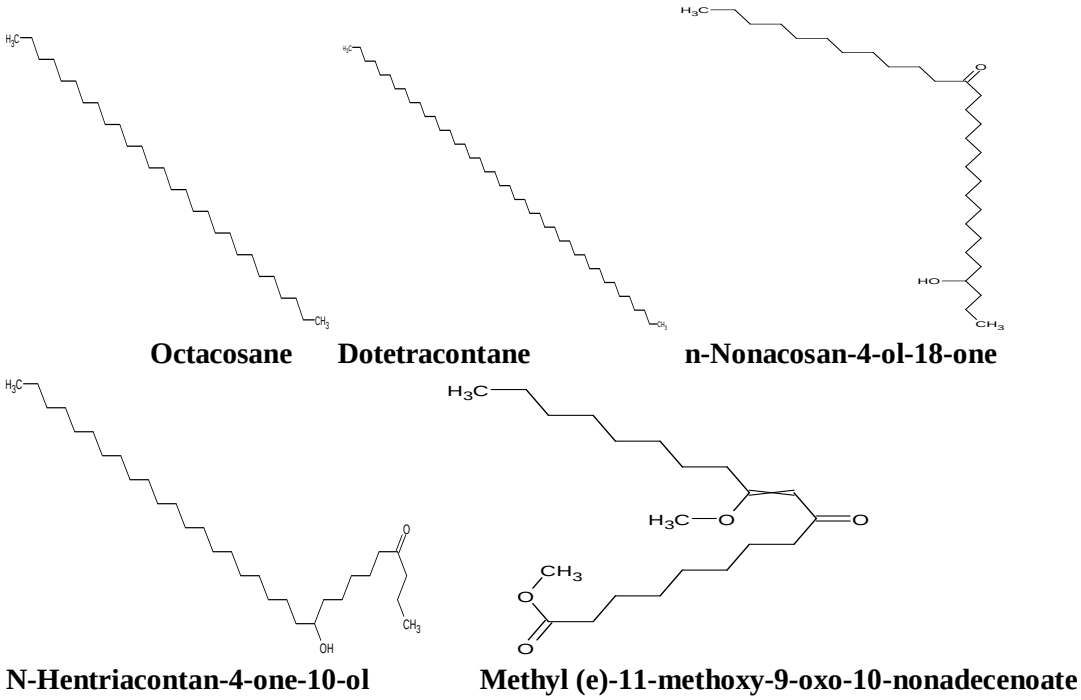

Figure 1.1 The 2D structure of phytochemical bioactive compounds

Analysis of Physiochemical Properties, Drug Likeness, and Pharmacokinetics Prediction

The pharmacokinetics properties (GI absorption, BBB permeation, P-gp substrate, cytochrome-P enzyme inhibition, log Kp) [15], and the physicochemical properties (molecular weight, TPSA, no. of HBD/no. of HBA, lipophilicity, and drug likeness (rule of five) were stated by SwissADME [16].

Toxicity prediction

The ProTox 3.0 server was used to determine the toxicity class and level of toxicity (LD50, mg/kg) as well as the toxicological endpoints (hepatotoxicity, neurotoxicity, nephrotoxicity, respiratory toxicity, cardiotoxicity, carcinogenicity, immunotoxicity, mutationagenicity, cytotoxicity, ecotoxicity, clinical toxicity, and nutritional toxicity) of the phytochemicals of *Hibiscus rosa sinensis* [17].

Protein Preparation

The RCSB Protein Data Bank provided the three-dimensional (3D) structures of TCF7L2 (PDB ID: 6od4) as receptor proteins in PDB format which are present in figure 1.2 [18].

Figure 1.2 Structure of Protein

Ligand Preparation

From the PubChem database, the 3D SDF files of every ligand molecules were obtained [14]. Using Pymol version 3.0.3, the SDF ligand files were converted to PDB format and 3D PDB file is finally converted to pdbqt format.

Molecular docking

The molecular docking was convey using AutoDock Tools v. 4.2.6 [19] and ligands were molecularly docked against the target protein TCF7L2 (PDB: 6od4) in relation to the receptor grid box. The pdbqt output file for the protein ligand was created once the RMSD value was determined.

Analysis of Protein-Ligand Interactions

Protein-ligand complexes were visualized and characterized using PyMOL software. PLIP was used to identify the receptor's active sites and its interactions with the ligand or drug [20].

RESULT AND DISCUSSION

Analysis of physicochemical properties and drug-likeness:-

Molecular weight, number of acceptor and donor hydrogen bonds, TPSA, and Log P are the physiochemical properties and drug similarity criteria listed in Table 1. Seven of the thirty-three physiochemical compounds found in *Hibiscus rosa sinensis* (dotetracontane, alpha-carotene, cyanin, quercetin 3-sophorotrioside, kaempferol, 3-xylosylglucoside, and quercetin-3, 7-diglucoside) do not violate Ro5 for oral bioavailability. It is crucial to remember that Ro5 is important to rational drug design, and it has been proposed that a compound's low permeability or poor absorption arises when one of the rules is violated .The ligand molecules should fall within this range in terms of mol. mass (g/mol) <500, calculated octanol/water partition coefficient (Log P) <5, no. of HBD <5, and no. of HBA <10, as per the rule of five.

In this study, we found that all phytoconstituents show a LogP value <5 except taraxerol acetate (12), alpha-caroten (17), hentriacontane (26), docosane (27), triacontane (28), octacosane (29), dotetracontane (30), n-Nonacosan-4-ol-18-one (31), and n-Hentriacontan-4-one-10-ol (32).Molecules with a TPSA of 140 Å2 and above would be poorly absorbed, with less than 10% of the molecules being absorbed fractionally and TPSA of 60 Å2 would be well absorbed 90% [29].The results also demonstrate an inverse relationship between TPSA and %Abs. All phytochemicals showed good intestinal absorption except Riboflavin (161.56 Å²), Cyanidin 3-sophoroside (161.56 Å²), Quercetin 3-diglucoside (289.66 Å²), Cyanin chloride (272.59 Å²), Kaempferol 3-xylosylglucoside (249.20 Å²), Quercetin-3, 7-diglucoside (289.66 Å²), Cyanin(272.59 Å²), Quercetin 3-sophorotrioside(368.81 Å²). The highest% absorption (99.9%) of phytoconstituents like taraxerol acetate, methyl malvalate, and methyl sterculate and the lowest% absorption (9.06%) of quercetin3-diglucoside,quercetin3,7-diglucoside, among thirty-three inquire phytoconstituents, according to an examination of the %Abs.

Table 1. The physicochemical Properties and drug-likeness of phytochemical compound

S NO.	Phytochemical Comp.	Mol. Wt. (g/mol)	No. of HBD	No. of HBA	log P	No. of rotable bond	TPSA (Å²)	% Absorption
1	Thiamine	265.35	2	3	-1.6	4	104.15	73
2	Riboflavin	376.36	5	8	0.97	5	161.56	53.2
3	Cyanidin 3-sophoroside	376.36	5	8	0.97	5	161.56	53.2
4	Sterculic acid	294.47	1	2	3.51	15	37.30	96.1
5	Malvalic acid	280.45	1	2	3.67	14	37.30	96.1
6	Flavylium	207.25	0	1	-0.76	1	13.14	104.4
7	Quercetin 3-diglucoside	626.52	11	17	0.9	7	289.66	9.06
8	Quercetin	302.24	5	7	1.63	1	131.36	63.6
9	D-Glucuronic Acid	194.14	5	7	-0.19	1	127.45	65
10	Ascorbic acid	176.12	4	6	0.39	2	107.22	72
11	Nicotinic acid	123.11	1	3	0.86	1	50.19	91.6
12	Taraxerol acetate	468.75	0	2	5.23	2	26.30	99.9
13	Cyanidin chloride	322.70	5	6	-4.55	1	114.29	69.5
14	Cyanin chloride	646.98	11	16	-4.3	7	272.59	14.9
15	Kaempferol 3-xylosylglucoside	580.49	9	15	2.39	7	249.20	23
16	Quercetin-3,7-diglucoside	626.52	11	17	2.06	7	289.66	9.06
17	alpha-Carotene	536.87	0	0	7.83	10	0.00	14.9
18	Cyanin	611.53	11	16	-5.96	7	272.59	
19	Stigmast-5-ene-3beta,4alpha-diol	430.71	2	2	4.72	6	40.46	95
20	beta-Sitosterol	430.71	2	2	4.72	6	40.46	95
21	D-Galactose	180.16	5	6	0.24	1	110.38	70
22	L-Rhamnose	180.16	4	5	0.66	0	90.15	77.8
23	Methyl malvalate	294.47	0	2	4.87	15	26.30	99.9
24	Methyl (e)-11-methoxy-9-oxo-10-nonadecenoate	354.52	0	4	4.92	18	52.60	90.8
25	Quercetin 3-sophorotrioside	788.66	14	22	1.85	10	368.81	18.2

26	Hentriacontane	436.84	0	0	8.25	28	0.00	109
27	Docosane	310.60	0	0	6.17	19	0.00	109
28	Triacontane	422.81	0	0	7.86	27	0.00	109
29	Octacosane	394.76	0	0	7.53	25	0.00	109
30	Dotetracontane	591.13	0	0	10.81	39	0.00	109
31	n-Nonacosan-4-ol-18-one	438.77	1	2	6.86	26	37.30	96.1
32	n-Hentriacontan-4-one-10-ol	466.82	1	2	7.42	28	37.30	96.1
33	Methyl sterculate	308.50	0	2	4.66	16	26.30	99.9

Pharmacokinetics properties

Candidate molecule toxicity and pharmacokinetics are the primary causes of drug development failure. Drugs' absorption, distribution, metabolism, excretion, and toxicity (ADMET) have been noted as crucial factors to take into account in the early phases of CADD. The GI of medications taken orally is established by both transit along the gastrointestinal tract and absorption through the gastrointestinal mucosa .To evaluate the absorption property of *Hibiscus rosa sinensis,* all thirty-three phytonstituents twelve of them show high gastrointestinal absorption, and the rest low gastrointestinal absorption. The BBB controls how permeable drugs are to the brain (Table 2). All of the phytoconstituents do not permeate BBB except malvalic acid (5), Flavylium (6), and nicotinic acid (11), using ADMET lab. For the treatment of diabetes mellitus, blood-brain barrier penetration is undesirable because it can cause side effects related to the CNS, so compounds that are able to penetrate the BBB are not preferred.A substance known as a p-glycoprotein substrate is one that makes use of the p-glycoprotein transporter for a variety of purposes, such as drug excretion and absorption.All of the thirty-three phytoconstituents sixteen of them show p-glycoprotein substrate activity and the rest of them do not show p-glycoprotein substrate activity (Table 2).

To identify cytochrome p450 inhibitory activities, such as CYP1A2, CYP2C19, CYP2C9, CYP2D6, and CYP3A4 inhibitors. Sterculic acid (4), Malvalic acid (5), Flavylium (6), Quercetin (8), Methyl malvalate (23), Docosane (27), and Methyl sterculate (33), were found to be inhibitors for CYP1A2. No inhibitors were found for CYP2C19 and CYP2C9 whereas Flavylium (6) Quercetin(8), were found inhibitors for CYP2D6. Quercetin (8) and Methyl (e)-11-methoxy-9-oxo-10-nonadecenoate (4) were found to be inhibitors for CYP3A4. The standard method for assessing the relevance of skin absorption for a target drug involves calculating the compound's skin permeability (Kp), also known as the skin ingress coefficient, in the stratum corneum. The rate of chemical ingress through the epidermal skin's outermost layer is quantitatively described by the Kp. All of the phytoconstituents contracted into consideration in this investigation had skin penetrability, or Kp value, that range from -0.01 to -13.12 cm/s (Table 2). It has been ensue that as

molecular size rises, log Kp increases (becomes more negative). The molecule is less skin permeant the lower the log Kp (with Kp measured in cm/s).

Table 2. The prediction of Pharmacokinetics properties of phytochemical compound

S. No.	Bioactive compounds	GI Absorption	BBB permeant	P-gp substrate	CYP1A2 inhibitors	CYP2C19 inhibitors	CYP2C9 inhibitors	CYP2D6 inhibitors	CYP3A4 inhibitors	LogKp (cm/s)
1	Thiamine	↑	×	✓	×	×	×	×	×	-7.19
2	Riboflavin	↓	×	×	×	×	×	×	×	-9.63
3	Cyanidin 3-sophoroside	↓	×	×	×	×	×	×	×	-11.07
4	Sterculic acid	↑	×	×	✓	×	×	×	×	-3.46
5	Malvalic acid	↑	✓	×	✓	×	×	×	×	-3.61
6	Flavylium	↑	✓	✓	✓	×	×	✓	×	-5.07
7	Quercetin 3-diglucoside	↓	×	×	×	×	×	×	×	-11.39
8	Quercetin	↑	×	×	✓	×	×	✓	✓	-7.05
9	D-Glucuronic Acid	↓	×	✓	×	×	×	×	×	-9.15
10	Ascorbic acid	↑	×	×	×	×	×	×	×	-8.54
11	Nicotinic acid	↑	✓	×	×	×	×	×	×	-6.80
12	Taraxerol acetate	↓	×	×	×	×	×	×	×	-2.14
13	Cyanidin chloride	↑	×	✓	×	×	×	×	×	-7.15
14	Cyanin chloride	↓	×	×	×	×	×	×	×	-11.69
15	Kaempferol 3-xylosylglucoside	↓	×	✓	×	×	×	×	×	-10.42
16	Quercetin-3,7-diglucoside	↓	×	✓	×	×	×	×	×	-11.14
17	alpha-Carotene	↓	×	✓	×	×	×	×	×	0.12
18	Cyanin	↓	×	✓	×	×	×	×	×	-12.05
19	Stigmast-5-ene-3beta,4alpha-diol	↓	×	×	×	×	×	×	×	-3.08
20	beta-Sitosterol	↓	×	×	×	×	×	×	×	-2.20
21	D-Galactose	↓	×	✓	×	×	×	×	×	-9.70
22	L-Rhamnose	↑	×	✓	×	×	×	×	×	-8.79
23	Methyl malvalate	↑	×	×	✓	×	×	×	×	-3.47
24	Methyl (e)-11-methoxy-9-oxo-10-nonadecenoate	↑	×	×	×	×	×	×	✓	-4.11
25	Quercetin 3-sophorotrioside	↓	×	✓	×	×	×	×	×	-13.12

26	Hentriacontane	↓	×	✓	×	×	×	×	×	2.69
27	Docosane	↓	×	×	✓	×	×	×	×	-0.01
28	Triacontane	↓	×	✓	×	×	×	×	×	2.39
29	Octacosane	↓	×	✓	×	×	×	×	×	1.79
30	Dotetracontane	↓	×	✓	×	×	×	×	×	5.97
31	n-Nonacosan-4-ol-18-one	↓	×	×	×	×	×	×	×	-0.73
32	n-Hentriacontan-4-one-10-ol	↓	×	✓	×	×	×	×	×	-0.13
33	Methyl sterculate	↑	×	×	✓	×	×	×	×	-3.23

Whereas; High=↑, Low=↓, Yes=✓, No= ×
GI=Gastro intestinal, BBB=Blood Brain Barrier, P-gp= p-Glycoprotein, logKp (skin permeation)

Toxicity Prediction

When choosing a plant as a potential medicinal candidate, one of the most crucial considerations is its absence of toxicity. The Web ProTox 3.0 servers provide a number of benefits over computer models. Information about chemistry, metabolism, molecular biology, and adverse effects (AOPs) can be found on the ProTox website. Herein, the toxicological endpoints and the level of toxicity (LD50, mg/kg) and toxicity class of the phytochemicals of *Hibiscus rosasinensis* were predicted. A natural or synthetic chemical can cause acute or chronic drug impel hepatotoxicity, often known as drug impel liver injury (DILI). The predicted descriptors are presented in Table 3. Nicotinic acid (11) is active for hepatotoxicity.The results demonstrate that thiamine (1), riboflavin (2), flavylium (6), nicotinic acid (11), taraxerol acetate (12), alpha-carotene (17), and beta-sitosterol (20) are active for neurotoxicity. Exogenous or endogenous toxicants can cause drug-induced nephrotoxicity when they come into contact with the kidney. Nephrotoxic medication exposure can impair the kidney's ability to keep the body's homeostasis stable. The results showed that Riboflavin(2), Cyanidin 3-sophoroside(3), Quercetin 3-diglucoside(7), Quercetin(8), D-Glucuronic Acid(9), Ascorbic Acid(10), Nicotinic Acid(11), Cyanidin chloride(13), Cyanin chloride(14), Kaempferol 3-xylosylglucoside(15), Quercetin-3,7-diglucoside(16), Cyanin(18), D-Galactose(21), L-Rhamnose(22), Methyl (e)-11-methoxy-9-oxo-10-nonadecenoate(24), Quercetin 3-sophorotrioside(25) are active for nephrotoxicity.

The results showed that Thiamine(1), Riboflavin(2), Cyanidin 3-sophoroside(3), Quercetin 3-diglucoside(7), Quercetin(8), Nicotinic acid(11), Taraxerol acetate(12), Cyanidin chloride(13), Cyanin chloride(14), Kaempferol 3-xylosylglucoside(15), Quercetin-3,7-diglucoside(16), Cyanin(18), Stigmast-5-ene-3beta,4-alpha-diol(19), beta-Sitosterol(20), Quercetin 3-sophorotrioside(25) are active for respiratory toxicity. Drug-induced cardiotoxicity can occur when the potassium ion channel known as the human ether-à-go-related gene (hERG) channel is inhibited. The hERG channel is crucial for regulating the cardiac action potential. The results also show round that all of the phytoconstituents are in active for cardiotoxicity except taraxerol acetate (12), cyanin chloride (14), D-galactose (21), and L-rhamnose (22). The result also show round that all of the phytoconstituents are not active for carcinogenicity except Flavylium (6), Quercetin (8), Taraxerol Acetate (12), and Stigmast-5-ene-3beta,4-alpha-diol (19).Acute toxicity is typically described by the term LD50, where LD stands for lethal dosage fatal amount and the subscript 50 indicates

that the dose is acutely lethal to 50% of the animals that were exposed to the chemical in a controlled laboratory setting. The findings indicated that the median fatal dose (LD50) ranged from 48 to 23000 mg/kg and toxicity class from 2-6 (Table 3).

Table 3. Pro Tox III stated organ toxicity, toxicological endpoints, and acute toxicity

S. No.	Phytoconstituents	Hepatotoxicity	Neurotoxicity	Nephrotoxicity	Respiratory Toxc.	Cardiotoxicity	Carcinogenicity	Immunotoxicity	Mutagenicity	Cytotoxicity	Ecotoxicity	Clinical Toxicity	Nutritional Toxc.	LD 50 (mg/kg)	Toxicity Class
1	Thiamine	00	00	00	00	00	00	00	00	00	00	00	00	1000	4
2	Riboflavin	00	00	01	01	00	00	00	00	00	00	01	00	10000	6
3	Cyanidin 3-sophoroside	00	00	01	01	00	00	01	00	00	00	00	01	5000	5
4	Sterculic acid	00	00	00	00	00	00	00	00	00	01	00	00	48	2
5	Malvalic acid	00	00	00	00	00	00	00	00	00	01	00	00	48	2
6	Flavylium	00	00	00	00	00	01	00	00	00	00	00	00	2500	5
7	Quercetin 3-diglucoside	00	00	01	01	00	00	01	00	00	00	01	01	5000	5
8	Quercetin	00	00	01	01	00	00	00	00	00	00	00	01	159	3
9	D-Glucuronic Acid	00	00	01	00	00	00	00	00	00	00	01	00	10000	6
10	Ascorbic acid	00	00	01	00	00	00	00	00	00	00	01	00	3367	5
11	Nicotinic acid	01	01	01	01	00	00	00	00	00	00	00	00	3720	5
12	Taraxerol acetate	00	00	00	00	01	01	01	00	00	01	00	00	3460	5
13	Cyanidin chloride	00	00	01	01	00	00	00	00	00	00	00	01	5000	5
14	Cyanin chloride	00	00	01	01	01	00	00	00	00	00	00	01	5000	5
15	Kaempferol 3-xylosylglucoside	00	00	01	01	00	00	01	00	00	00	00	01	5000	5
16	Quercetin-3,7-diglucoside	00	00	01	01	00	00	01	00	00	00	01	01	5000	5
17	alpha-Carotene	00	00	00	00	00	00	00	01	00	00	00	00	1510	4
18	Cyanin	00	00	01	01	00	00	01	00	00	00	00	01	5000	5

19	Stigmast-5-ene-3beta,4alpha-diol	00	00	00	01	00	00	01	00	00	01	01	01	2000	4
20	beta-Sitosterol	00	01	00	01	00	00	01	00	00	01	00	00	890	4
21	D-Galactose	00	00	01	00	01	00	00	00	00	00	00	00	23000	6
22	L-Rhamnose	00	00	01	00	01	00	00	00	00	00	01	00	23000	6
23	Methyl malvalate	00	00	00	00	00	00	00	00	00	01	00	00	3000	5
24	Methyl (e)-11-methoxy-9-oxo-10-nonadecenoate	00	00	01	00	00	00	00	00	00	00	00	00	4460	5
25	Quercetin 3-sophorotrioside	00	00	01	01	00	00	01	00	00	00	01	01	5000	5
26	Hentriacontane	00	00	00	00	00	00	00	00	00	01	00	00	750	3
27	Docosane	00	00	00	00	00	00	00	00	00	01	00	00	750	3
28	Triacontane	00	00	00	00	00	00	00	00	00	01	00	00	750	3
29	Octacosane	00	00	00	00	00	00	00	00	00	01	00	00	750	3
30	Dotetracontane	00	00	00	00	00	00	00	00	00	01	00	00	750	3
31	n-Nonacosan-4-ol-18-one	00	00	00	00	00	00	00	00	00	01	00	00	750	3
32	n-Hentriacontan-4-one-10-ol	00	00	00	00	00	00	00	00	00	01	00	00	5000	5
33	Methyl sterculate	00	00	00	00	00	00	00	00	00	01	00	00	3000	5

Whereas, Inactive= 00, Active=01

Molecular docking

Molecular docking aims to accurately admeasure the intensity of ligation and predict the structure of a ligand within the bounds of a receptors binding site. Following the conclusion of the docking experiment, 17 out of the 33 phytoconstituents exhibit ligand-pose interaction. The result of the docking analysis of the 17 best phytoconstituents is described in Table 4.The aim of the study was to conjecture the binding affinity of seventeen phytoconstituents to the target protein, i.e., TCF7L2. The phytoconstituents under analysis showed binding energies between -8.04 and -2.85 kcal/mol, which have been represented in figure 1.3. The caput six phytoconstituents with low binding energies were beta-sitosterol, stigmast-5-ene-3beta, 4alpha-diol, Flavylium, quercetin, alpha-Carotene and Thiamine.

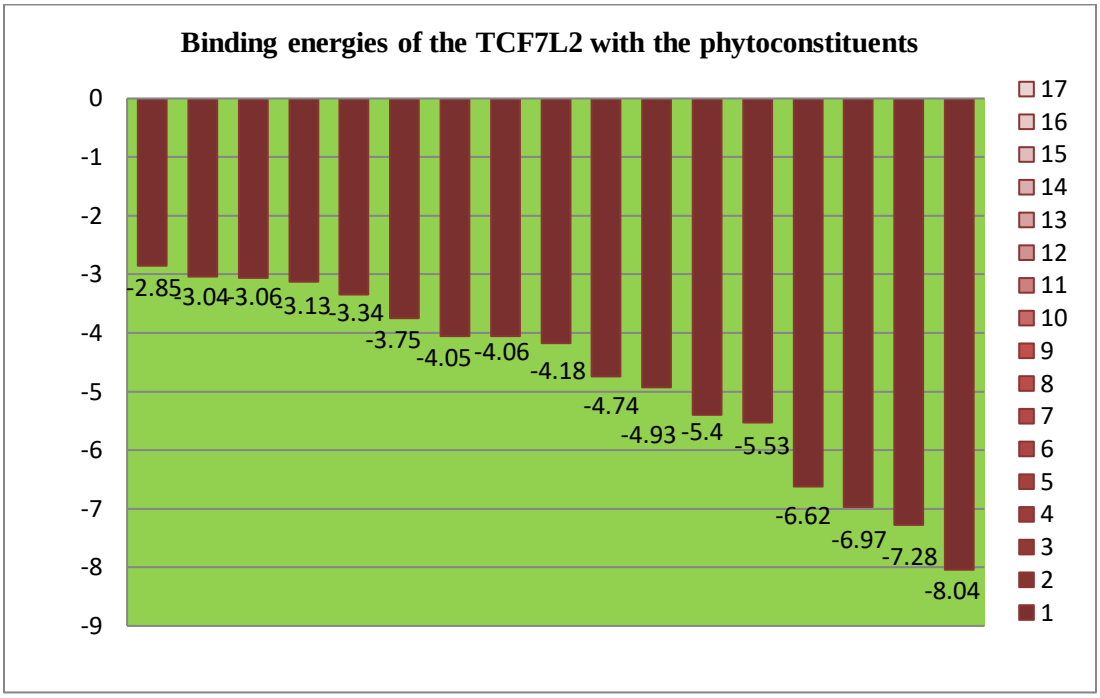

Figure. 1.3 Graphical remonstrant of binding energies of the phytoconstituents with TCF7L2

Visualization of Ligand- Protein interaction

The interaction between the ligand and protein was visualized using PLIP to confirm site-specific ligand binding. The interplay like hydrogen bonds, hydrophobic bonds, salt bridges, and active amino acid residues responsible for the formation of the active site are predicted and summarized in Table 4. Based on past docking studies, the greater the number of hydrogen bond interplay, the stronger the interplay between the ligand and the active site of the protein.Overall, the *in silico* docking analysis indicated that beta-sitosterol does not interact with hydrogen bonding and two hydrophobic and other interacting residues (PRO- 604B, THR-606B), Stigmast-5-ene-3beta,4-alpha-diol did not find any interaction with the hydrogen bond, one hydrophobic residue, or other interacting residues (ILE-610A).

Quercetin formed hydrogen bond reciprocity with two amino acid residuum (ASN-573B, GLU-577B) and two hydrophobic and other interacting residues (ASN-573B, ARG-576B), alpha-carotene formed hydrogen bond interactions with four amino acid residues of the active site, including GLU-590G, HIS-612H, SER-620H, and GLN-623H, and two hydrophobic and other interacting residues (LEU-619H, HIS-612H) and Thiamine formed two hydrogen bond interactions with amino acid residues (GLU-577B, ASP-583) and one hydrophobic and other interacting residue (ARG-580B).The docked position amino acid residues include salt bridges, hydrophobic bonds, and hydrogen bond interactions of phytoconstituents with TCF7L2 was generated through the PyMOL tool (Fig. 1.4).

Table 4. Binding energy and Molecular docking interactions of TCF7L2 with the phytoconstituents

S. No.	Phytoconstituents	Binding Energy (kcal/mol)	Hydrogen bond interaction	Hydrophobic and other interaction
1	beta-Sitosterol	-8.04	----------	PRO- 604B,THR-606B
2	Stigmast-5-ene-3beta,4alpha-diol	-7.28	----------	ILE-610A
3	Flavylium	-6.97	----------	ASN-573B,ARG-576B,ARG-580B
4	Quercetin	-6.62	ASN- 573B, GLU-577B	ASN-573B, ARG-576B
5	alpha-Carotene	-5.53	GLU- 590G,HIS-612H,SER-620H , GLN-623H	LEU-619H, HIS-612H
6	Thiamine	-5.4	GLU-577B, ASP- 583B	ARG-580B
7	Riboflavin	-4.93	ASN- 573B	LEU-619H
8	Cyanin	-4.74	ASN-585A,GLN-605A	----------
9	L-Rhamnose	-4.18	THR-606A, LYS-607A, LEU-608A	ASP- 583B, LEU-608A,
10	D-Galactose	-4.06	ARG-580A, ARG-580B,LYS-607A,LYS-607B	LYS-607A
11	Quercetin-3,7-diglucoside	-4.05	ARG-576B, ARG-580B, GLU-590G, ARG-593G	GLU-590G, VAL-615H, LEU-619H, ARG- 593G
12	Docosane	-3.75	----------	ARG-580B,ASP-583G, ILE-584B,GLU-586G,ALA-587G,LYS-603A,THR-606A, LEU-608A, LEU- 608H, VAL-615H
13	Hentriacontane	-3.34	----------	LEU-579B, LEU-579G, ARG-580B, ALA-587G, LEU-599A, SER-601A, LYS-603A, THR-606A, LEU-608A, LEU-608H, LEU-609A, HIS-612H, GLN-613A
14	Triacontane	-3.13	----------	PHE-588A, LYS-589A, ARG-593A, GLN-605A, LYS-607A, ILE-610A

15	n-Hentriacontan-4-one-10-ol	-3.06	GLN-623H	ARG-580B, LYS-603A, LEU-608A, LEU-608H, LEU-609A, HIS-612H, LEU-619H
16	n-Nonacosan-4-ol-18-one	-3.04	GLN-605A	LYS-589A, PRO-604A, GLN-605A, THR-606A, ILE-610A
17	Octacosane	-2.85	----------	PRO-604A, ALA-616H

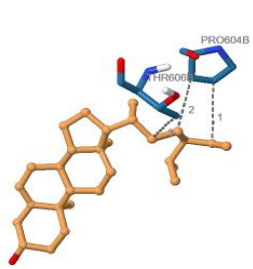

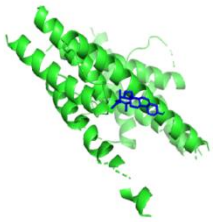

1 **2**

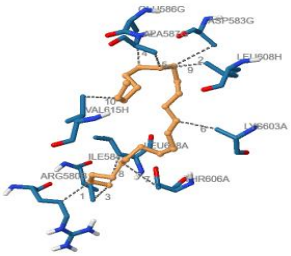

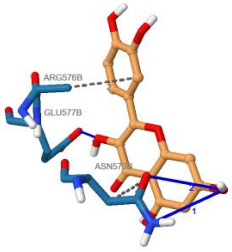

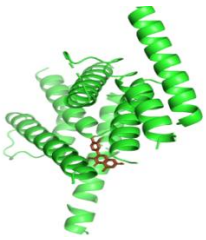

3 **4**

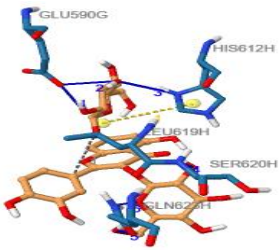

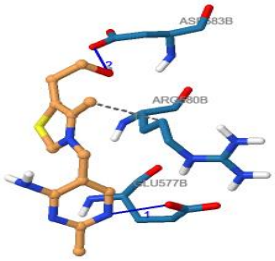

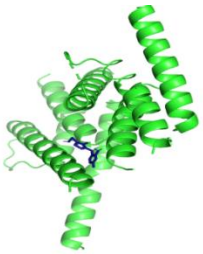

5 **6**

Where as;

-Protein - Ligand - Water Charge center& salt bridge

- Aromatic ring center - Hydrogen bond - Hydrophobic interaction

Figure 1.4-D views of the interaction between ligand (phytoconstituents) and target protein (TCF7L2) and amino acid residues include hydrogen bond, hydrophobic bonds and other interactions of proiein & ligand The numbers (1 to 6) stand for (1) beta-Sitosterol,(2) Stigmast-5-ene-3beta,4alpha-diol,(3) Flavylium,(4) Quercetin,(5) alpha-Carotene,(6) Thiamine. The colour of protein is represented by green and ligand is represented by different colour.

CONCLUSION

Using *in silico* methods, the thirty-three phytoconstituents pin down from the plants were stated for their inhibitory actions against diabetes mellitus. Compounds from *Hibiscus rosa sinensis* that have the best binding affinity protein targets were beta-sitosterol (8.04 kcal/mol), stigmast-5-ene-3beta, 4-diol (-7.28kcal/mol), flavylium (6.97 kcal/mol), quercetin (6.62 kcal/mol), alpha-Carotene (-5.53 kcal/mol) and Thiamine to TCE7L2 (-5.4kcal/mol) , beta-Sitosterol, Stigmast-5-ene-3beta, 4alpha-diol and alpha-Carotene have best binding energy but low GI Absorption. Quercetin have high GI Absorption but toxic if swallowed. Based on a study that predicts toxicological endpoints, the median fatal dosage (LD50) ranges from 48 to 23000 mg/kg. Subsequent analysis of the ligand-protein interactions, physiochemicals, ADMET, and drug-likeness factors revealed that flavylium, Quercetin and thiamine had encouraging characteristics and might serve as a viable therapeutic candidate.

FUTURE PROSPECTIVE

Further in vivo and in vitro research to determine the most suitable medicinal molecule Flavylium, Quercetin and thiamine would be based on the predictions regarding the molecular docking, drug likeness, pharmacokinetic and toxicity features of these phytoconstituents.

Acknowledgements

I am incredibly appreciative of Dr. OP Verma, Head of the Pharmacy Department, Goel Institue of Pharmacy & Sciences, Lucknow, for his encouragement and assistance. With great pleasure, I would like to pour out my appreciation to my supervisor, Mr. Salil Tiwari, an associate professor in the pharmacy department of Goel Institue of Pharmacy & Sciences, Lucknow and co-supervisor, Ms. Nootan Singh Senior scientist, Experiome Biotech Private Limited, Lucknow. His unwavering counsel, creative ideas, and unceasing encouragement and monitoring are all readily available to me while I make the necessary arrangements to finish my dissertation.

I owe a debt of gratitude to my parents and relatives beyond everything else, as their unfailing love, support, and faith in my abilities have been my inspiration. My deepest gratitude goes out to my seniors and my dear friends.

Conflict of interest

All the authors' promuglate that there is no conflict of interest.

REFERENCE

1. A. Mishra, G. Dewangan, T. K. Mandal, & J. Chkraborty, LD_{50} dose fixation of nanohybrid-layered double hydroxide-methotrexate. *Indian journal of pharmacology*, *54*(5), **(2022)**, pp. 379–380.
2. J. B. Cole, &J. C. Florez, Genetics of diabetes mellitus and diabetes complications. Nature reviews nephrology, 16(7), **(2020)**, pp, 377-390.

3. Y. Sun, Q.Tao, X.Wu, L. Zhang, Q. Liu, & L. Wang, The Utility of Exosomes in Diagnosis and Therapy of Diabetes Mellitus and Associated Complications. *Frontiers in endocrinology*, *12*, 756581**(2021).**
4. M. K. Ali, J. Pearson-Stuttard, E. Selvin, & E. W. Gregg, Interpreting global trends in type 2 diabetes complications and mortality. *Diabetologia*, *65*(1), **(2022),** pp.3–13.
5. L. Del Bosque-Plata, E. Martínez-Martínez, M. Á. Espinoza-Camacho, & C. Gragnoli, The Role of *TCF7L2* in Type 2 Diabetes. *Diabetes*, *70*(6), **(2021)**,-pp. 1220–1228.
6. J. J. Mejía, , L. J. Sierra, , J. G. Ceballos, J. R. Martínez, & E. E. Stashenko, Color, Antioxidant Capacity and Flavonoid Composition in *Hibiscus rosa-sinensis* Cultivars. *Molecules (Basel, Switzerland)*, *28*(4), 1779, **(2023).**
7. H. H. Lan, & L. M. Lu, Characterization of Hibiscus Latent Fort Pierce Virus-Derived siRNAs in Infected *Hibiscus rosa-sinensis* in China. *The plant pathology journal*, *36*(6), (**2020)**,pp. 618–627.
8. OH Abdelhafez, EM Othman, JR Fahim, SY Desoukey, SM Pimentel-Elardo, JR. Nodwell et al. Metabolomics analysis and biological investigation of three Malvaceae plants. Phytochem. Anal.; 31: **(2020)** ,pp. 204-214
9. S. Amtaghri, A. Qabouche., M. Slaoui,, & M. Eddouks, A Comprehensive Overview of *Hibiscus rosa-sinensis* L.: Its Ethnobotanical Uses, Phytochemistry, Therapeutic Uses, Pharmacological Activities, and Toxicology. *Endocrine, metabolic & immune disorders drug targets*, *24*(1), **(2024) ,** pp. 86–115.
10. P. Ansari,, S. Azam,, J. M. A. Hannan,, P. R. Flatt,, & Y. H. A. Abdel Wahab, Anti-hyperglycaemic activity of H. rosa-sinensis leaves is partly mediated by inhibition of carbohydrate digestion and absorption, and enhancement of insulin secretion. *Journal of ethnopharmacology*, *253*, 112647 **(2020).**
11. G. Xiong,, Z. Wu,, J. Yi,, L. Fu,, Z. Yang,, C. Hsieh,, M. Yin,, X. Zeng, C. Wu, A. Lu, X. Chen, T. Hou, & D. Cao, ADMETlab 2.0: an integrated online platform for accurate and comprehensive predictions of ADMET properties. *Nucleic acids research*, *49*(W1), W5–W14, **(2021).**
12. R.M. Stein, H.J. Kang, J.D. McCorvy, G.C. Glatfelter, A.J. Jones, T. Che, S. Slocum, X.-P. Huang, O. Savych, Y.S. Moroz, Virtual discovery of melatonin receptor ligands to modulate circadian rhythms. *Nature*; 579:, (**2020)** ,pp.609–614.
13. F. Stanzione, I. Giangreco, & J. C. Cole, Use of molecular docking computational tools in drug discovery. *Progress in medicinal chemistry*, *60*, **(2021)** , pp.273–343.
14. S Kim, J Chen, T Cheng, A Gindulyte, J He, He S, Li Q, BA Shoemaker, PA Thiessen, Yu B, L Zaslavsky, J Zhang, and EE Bolton PubChem in 2021: New data content and improved web interfaces. Nucleic Acids Res 49:D **(2021)**, pp.1388–D1395.
15. O. O. Olaokun, & M. S. Zubair, Antidiabetic Activity, Molecular Docking, and ADMET Properties of Compounds Isolated from Bioactive Ethyl Acetate Fraction of *Ficus lutea* Leaf Extract. *Molecules (Basel, Switzerland)*, *28*(23), **(2023)**, pp. 7717.
16. G Xiong, Z Wu, J Yi, L Fu, Z Yang, C Hsieh, M Yin, X Zeng, C Wu, A Lu, X Chen, T Hou, D Cao ADMETlab 2.0: An integrated online platform for accurate and comprehensive predictions of ADMET properties. Nucleic Acids Res 49:W5–W14 (**2021).**
17. L. Luo, A. Zhong, Q. Wang, & T. Zheng, Structure-Based Pharmacophore Modeling, Virtual Screening, Molecular Docking, ADMET, and Molecular Dynamics (MD) Simulation of Potential Inhibitors of PD-L1 from the Library of Marine Natural Products. *Marine drugs*, *20*(1), (**2021)**, pp.29.
18. S. K. Burley, C. Bhikadiya, C. Bi, S. Bittrich, L. Chen, G. V. Crichlow, J. M. Duarte,S. Dutta, M. Fayazi, Z. Feng, J. W. Flatt, S. J. Ganesan, D. S. Goodsell, S. Ghosh, R. Kramer Green, V. Guranovic, J Henry, B. P. Hudson, C. L. Lawson, Y. Liang, C. Zardecki, RCSB Protein Data Bank: Celebrating 50 years of the PDB with new tools for understanding and visualizing biological macromolecules in 3D. *Protein science: a publication of the Protein Society*, *31*(1), **(2022)**,pp.187–208.
19. D. S. Goodsell, M. F. Sanner, A. J. Olson, & S. Forli, the AutoDock suite at 30. *Protein science: a publication of the Protein Society*, *30*(1), **(2021)**, pp.31–43.
20. W. Luo, J. Deng, J. He, L. Yin, R. You, L. Zhang, J. Shen, Z. Han, F. Xie, J. He, & Y. Guan, Integration of molecular docking, molecular dynamics and network pharmacology to explore the multi-target pharmacology of fenugreek against diabetes. *Journal of cellular and molecular medicine*, *27*(14), **(2023)**, pp. 1959–1974.